

Investigate small particles with unparalleled sensitivity
Amnis® CellStream® Flow Cytometry System

For Research Use Only. Not for use in diagnostic procedures.



Luminex®
complexity simplified.



Quantifying the Contribution of Defective Ribosomal Products to Antigen Production: A Model-Based Computational Analysis

This information is current as of August 16, 2022.

Sascha Bulik, Bjoern Peters and Hermann-Georg Holzhütter

J Immunol 2005; 175:7957-7964; ;
doi: 10.4049/jimmunol.175.12.7957
<http://www.jimmunol.org/content/175/12/7957>

References This article **cites 40 articles**, 16 of which you can access for free at:
<http://www.jimmunol.org/content/175/12/7957.full#ref-list-1>

Why *The JI*? [Submit online.](#)

- **Rapid Reviews! 30 days*** from submission to initial decision
- **No Triage!** Every submission reviewed by practicing scientists
- **Fast Publication!** 4 weeks from acceptance to publication

**average*

Subscription Information about subscribing to *The Journal of Immunology* is online at:
<http://jimmunol.org/subscription>

Permissions Submit copyright permission requests at:
<http://www.aai.org/About/Publications/JI/copyright.html>

Email Alerts Receive free email-alerts when new articles cite this article. Sign up at:
<http://jimmunol.org/alerts>

The Journal of Immunology is published twice each month by
The American Association of Immunologists, Inc.,
1451 Rockville Pike, Suite 650, Rockville, MD 20852
Copyright © 2005 by The American Association of
Immunologists All rights reserved.
Print ISSN: 0022-1767 Online ISSN: 1550-6606.



Quantifying the Contribution of Defective Ribosomal Products to Antigen Production: A Model-Based Computational Analysis

Sascha Bulik,* Bjoern Peters,[†] and Hermann-Georg Holzhütter^{1*}

Antigenic peptides (epitopes) presented on the cell surface by MHC class I molecules derive from proteolytic degradation of endogenous proteins. Some recent studies have proposed that the majority of epitopes stem from so-called defective ribosomal products (DRiPs), i.e., freshly synthesized proteins that are unable to adopt the native conformation and thus undergo immediate degradation. However, a reliable computational analysis of the data underlying this hypothesis was lacking so far. Therefore, we have applied kinetic modeling to derive from existing kinetic data (*Princiotta et al. 2003, Immunity 18, 343–354*) the rates of the major processes involved in the cellular protein turnover and MHC class I-mediated Ag presentation. From our modeling approach, we conclude that in these experiments 1) the relative share of DRiPs in the total protein synthesis amounted to ~10% thus being much lower than reported so far, 2) DRiPs may become the decisive source of epitopes within an early phase after onset of the synthesis of a long-lived (e.g., virus derived) protein, and 3) inhibition of protein synthesis by the translation inhibitor cycloheximide appears to be paralleled with an instantaneous decrease of protein degradation down to ~1/3 of the normal value. *The Journal of Immunology, 2005, 175: 7957–7964.*

In mammalian cells, most cellular proteins undergo a continual turnover, which is driven by synthesis at the ribosomes and degradation by proteasomes or lysosomal proteases (1). This turnover allows a flexible adaptation of protein levels to varying specific functions of the cell. The protein synthesizing and degrading machineries have sufficient excess capacity to cope with various forms of physical or chemical stress that require a rapid increase of the protein turnover. Moreover during their life span, proteins may experience diverse chemical modifications that alter their structure and thus their functional capabilities. Degradation of impaired proteins is a necessary prerequisite for the maintenance of cellular integrity.

The majority of cellular proteins are degraded via the ubiquitin-proteasome pathway that involves two steps: addition of a chain of ubiquitin molecules to an internal lysine side chain of a target protein and proteolysis of the ubiquitinated protein by the proteasome, a large, cylindrical multisubunit complex (2). The numerous proteasomes present in the cell cytosol proteolytically cleave ubiquitin-tagged proteins in an ATP-dependent process that yields peptides with varying lengths between 3 and 25 residues (3, 4) or even longer (5). Most of these fragments are further degraded into free amino acids by the action of various cytosolic proteases. In higher eukaryotes, some proteolytic fragments escape into the endoplasmic reticulum (ER)² where they may form a complex with MHC class I receptor molecules that is transported to the cell surface along the

vesicular pathway (6). Cytotoxic T lymphocytes are able to identify and attack those body cells presenting on their surface “foreign” antigenic peptides that do not derive from the pool of proteins normally produced in intact cells. Such abnormal proteins may occur in a malignant cell or after infection of the cell by a pathogen (e.g., virus).

The life span of intracellular proteins varies from as short as a few minutes for mitotic cyclins, which help regulate passage through mitosis, to as long as the age of an organism for proteins in the lens of the eye. The so-called N-end rule relates the in vivo half-life of a protein to the identity of its N-terminal residue (7). For example, in yeast *Saccharomyces cerevisiae*, the half-life of chimeric proteins composed of ubiquitin and a reporter protein such as β -galactosidase could be reduced from several hours to ~3 min by replacing a stabilizing N-terminal residue such as Thr or Ala by a destabilizing residue such as Arg or Lys (8). The large differences in the life span of individual proteins imply corresponding differences in the time delay between onset of a protein’s synthesis and appearance of an antigenic peptide contained within it. Indeed, investigating the effect on MHC class I Ag presentation of enhancing a protein’s rate of degradation by the ubiquitin-proteasome pathway, Grant et al. (9) demonstrated that the rate of presentation of microinjected β -galactosidase was enhanced when this antigenic protein was modified with a destabilizing amino-terminal residue. On the other hand, Groettrup and coworkers (10) demonstrated that selective inhibition of the cellular synthesis of a viral nucleoprotein (NP) with a half-life >3 days almost instantaneously ceased the production of an immunodominant epitope derived from this protein. This observation fits well to the hypothesis that irrespective of the half-life of a native protein there exists a certain fraction of newly synthesized proteins that undergo immediate degradation within several minutes (11, 12). This extremely labile fraction of proteins is commonly referred to as defective ribosomal products (DRiPs) to indicate that these polypeptides fail to adopt their native structure owing to errors in translation or posttranslational processes necessary for proper protein folding. It is even possible that nascent peptide chains still attached to the ribosome are cotranslationally degraded and thus have to be assigned to the DRiP pool (12).

*Institut für Biochemie, Charité, Humboldt Universität, Berlin, Germany; and [†]La Jolla Institute for Allergy and Immunology, San Diego, CA 92121

Received for publication June 3, 2005. Accepted for publication September 27, 2005.

The costs of publication of this article were defrayed in part by the payment of page charges. This article must therefore be hereby marked *advertisement* in accordance with 18 U.S.C. Section 1734 solely to indicate this fact.

¹ Address correspondence and reprint requests to Dr. Hermann-Georg Holzhütter, Humboldt Universität, Medizinische Fakultät (Charité), Institut für Biochemie, Monbijoustrasse 2, D-10117 Berlin, Germany. E-mail address: hergo@charite.de

² Abbreviations used in this paper: ER, endoplasmic reticulum; DRiP, defective ribosomal product; NP, nucleoprotein; R-NP, recombinant NP with Arg as N-terminal residue.

On one hand, the production of DRiPs means a waste of the protein-synthesizing capacity. On the other hand, it shortens the time gap between protein synthesis and Ag presentation and thus may allow for an instantaneous immune response even if the epitope-delivering protein is long-lived. This might be of particular relevance in cells that are infected by a virus because most virus proteins possess long half-lives of several days (13). The idea that epitopes derive predominantly from newly synthesized proteins received further support from the observation that the cellular concentration of peptides rapidly declines after complete inhibition of protein synthesis (14).

Examining the available experimental studies on the cellular production of DRiPs and their relevance as a source of antigenic peptides, two critical remarks have to be made. First, what these studies have actually demonstrated is the existence of a short-lived fraction of an otherwise stable native protein. However, that this short-lived fraction called DRiPs is really constituted by abnormal or nonfunctional polypeptide chains remains to be demonstrated. In that respect, it would have been better to denote this labile fraction with the acronym IDRiPs (immediately degraded ribosomal products). Second, a quantitative analysis of the so-called DRiP rate, i.e., the relative share of DRiPs in the total protein production of the cell is still lacking. An estimate like “upwards 35%” can be found in several papers (11, 15, 16), but this figure represents only a rough estimate and was not based on a quantitative analysis of the underlying data. An accurate estimate of DRiP rates actually present under different experimental conditions is necessary, however, to address the following important issues: 1) Are DRiPs a more or less fixed fraction of newly synthesized proteins or may their relative rate vary? 2) To what extent do DRiPs actually increase the efficiency of Ag presentation within the transient period following the onset of the synthesis of a novel protein?

To answer these questions on the basis of reliable quantitative measures, we have applied kinetic modeling to reanalyze a cardinal experiment supporting the so-called DRiP hypothesis. The experiment consisted in the transfection of various GFP-tagged chimeric protein constructs with different half-lives into L929 cells (16). The protein constructs harbored the antigenic peptide SIINFEKL. Monitoring simultaneously the time courses of intracellular protein levels and appearance of SIINFEKL class I complexes on the cell surface, the authors concluded that the antigenic peptide was more efficiently derived from the short-lived construct.

In the following, we outline the formulation of the kinetic model and the results obtained by comparing model simulations with data from the above mentioned experiments.

Materials and Methods

Background/experimental data

In brief, the experiment consisted in the simultaneous time-dependent monitoring of the intracellular copy numbers of a transfected GFP-tagged protein and the copy numbers of a presented Ag (SIINFEKL) excised from this protein. Several protein constructs with differing half-lives (see Table I) were used in these transfection experiments with L929 cells. To discriminate between the fractions of the antigenic peptide deriving either from the pool of native proteins or DRiPs, protein synthesis was blocked by addition of cycloheximide at 140 min after onset of transfection. Further details of the experiments are given in the legend to Fig. 2.

Table I. Chimeric protein constructs for which model simulations were performed and compared with kinetic data given by Princiotta et al. (16)

Name	Composition	Reported Half-Life
NP-GFP	NP-SIINFEKL-EGFP	Several hours
R-NP-GFP	Ub-R-NP-SIINFEKL-EGFP	≈10 min
KEKE-NP-GFP	NP-KEKE-SIINFEKL-EGFP	≈70 min

Kinetic model

The kinetic model used to simulate the experiments subdivides the polypeptides translated from one and the same mRNA into two classes: 1) native proteins that after folding carry a nonfluorescent GFP tag that after some time delay becomes fluorescent; and 2) DRiPs that are unable to fold into the native conformation and thus may not carry a fluorescent GFP tag. Both classes of proteins can be synthesized and degraded with different rates. The reactions steps included in the model are shown in Fig. 1: 1) synthesis and degradation of the mRNA for a specific transfected protein; 2) translation of the native protein and of DRiPs from the mRNA; 3) activation of the reporting molecule (here the GFP) after synthesis of the native protein; 4) proteolytic degradation of the native protein and DRiPs whereby the presented antigenic peptide (SIINFEKL) can be generated from the native protein as well as from DRiPs; and 5) appearance of the antigenic peptide (SIINFEKL) at the cell surface. For the kinetics of these reactions, we used simple first-order rate equations:

$$\frac{d}{dt}[\text{mRNA}] = v_0 - b_0[\text{mRNA}]$$

$$\frac{d}{dt}[\text{DRiP}] = \Theta (T_c - t)k_{21}[\text{mRNA}] - a_1[\text{DRiP}]$$

$$\frac{d}{dt}[\text{GFP}] = \Theta (T_c - t)k_{22}[\text{mRNA}] - (k_3 + a_2)[\text{GFP}]$$

$$\frac{d}{dt}[\text{XGFP}] = k_3[\text{GFP}] - a_2[\text{XGFP}]$$

$$\frac{d}{dt}[\text{SIINFEKL}] = \eta a_1[\text{DRiP}(t - \tau)] + \eta a_2([\text{GFP}(t - \tau)] + [\text{XGFP}(t - \tau)])$$

$$\Theta(x) = \begin{cases} 1 & \text{if } x \geq 0 \\ 0 & \text{else} \end{cases} \quad (1)$$

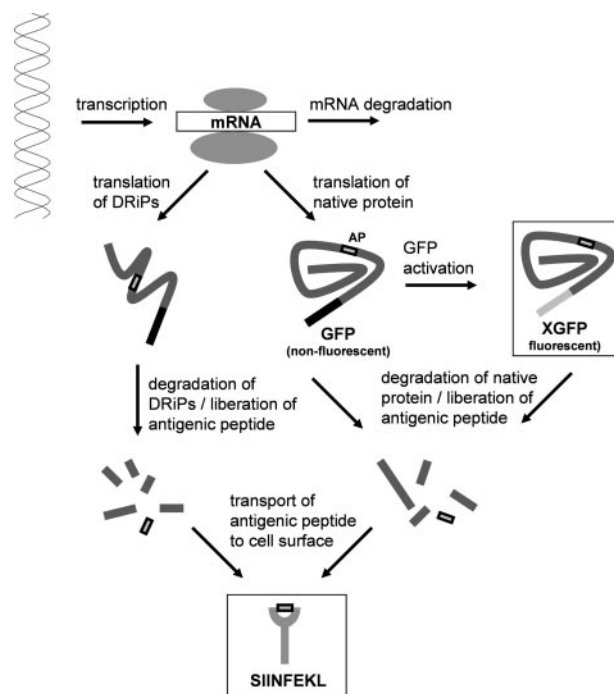


FIGURE 1. Simplified reaction scheme for the cellular protein turnover and MHC class I-mediated Ag presentation. Variables: mRNA, messenger RNA of a specific protein transfected into the cell; DRiP, DRiP translated from the mRNA; GFP, nonvisible GFP-tagged native protein (GFP not fluorescent); XGFP, visible GFP-tagged native protein (GFP fluorescent); SIINFEKL, presented antigenic peptide excised from the transfected protein. Note that the various proteolytic processes leading to a loss of epitopes or epitope precursors are not shown in this scheme but are implicitly included in the model by the parameter “presentation efficiency.”

The first equation of system (1) describes the time-dependent evolution of the mRNA concentration being the net balance of synthesis with constant transcription rate v_0 and a first-order decay occurring with rate constant b_0 . The second and third equation describe the time evolution of the DRiP fraction and the native (folded but nonfluorescent) protein. k_{21} , a_1 and k_{22} , a_2 denote the elementary rate constants for the synthesis and proteolytic degradation of these two different protein pools. The rate of protein synthesis is set to be proportional to the concentration of the messenger RNA. The unit-step function $\Theta(X)$ indicates that the rate of protein synthesis is put to zero for times $t \geq T_c$ where T_c indicates the time point at which an inhibitor of protein synthesis is added. The fourth equation describes the time evolution of the observable (= fluorescent) native protein with k_3 being the rate constant for the transition from the nonfluorescent to the fluorescent form of GFP. We assume that the degradation rate of the native protein is not influenced by the activation state of the GFP moiety so that for both types of GFP-tagged native protein the same degradation rate constant a_2 can be used. The last equation in system (1) describes the time-dependent number of epitopes on the cell surface. The parameter τ refers to the time delay between the proteolytic generation of the peptide in the cytosol and its arrival on the cell surface. For the time scale considered in the simulated experiments, the removal of antigenic peptides from the cell surface can be neglected and thus was not included in the model.

One crucial parameter of the model is the presentation efficiency η ($0 \leq \eta \leq 1$) of the antigenic peptide (here SIINFEKL). The presentation efficiency has the meaning of a probability with which degradation of a single protein harboring a specific epitope gives rise to the appearance of this epitope on the cell surface. This probability is equivalent to the inverse of the average number of proteins that have to be degraded to yield a single presented antigenic peptide.

The linear differential equation system (1) can be solved analytically. Assuming that at time $t = 0$ the concentration of all variables was zero (initial conditions) the time dependence of the model variables mRNA, DRiP, GFP, XGFP, and SIINFEKL are given as follows:

Without inhibition of protein synthesis ($t \leq T_c$)

$$\begin{aligned}
 \text{mRNA}(t) &= \frac{v_0}{b_0} [1 - \exp(-b_0 t)] \\
 \text{DRiP}(t) &= k_{21} v_0 \left[\frac{1 - \exp(-a_1 t)}{a_1 (b_0 - a_1)} + \frac{1 - \exp(-b_0 t)}{b_0 (a_1 - b_0)} \right] \\
 \text{GFP}(t) &= \frac{k_{22} v_0}{(a_2 + k_3 - b_0)} \left[\frac{1 - \exp(-b_0 t)}{b_0} - \frac{1 - \exp(-(a_2 + k_3)t)}{(a_2 + k_3)} \right] \\
 \text{XGFP}(t) &= \frac{k_{22} k_3 v_0}{(a_2 + k_3 - b_0)} \left[\frac{a_2 + k_3 - b_0}{a_2 k_3 (b_0 - a_2)} [1 - \exp(-a_2 t)] + \frac{1 - \exp(-(a_2 + k_3)t)}{k_3 (a_2 + k_3)} + \frac{1 - \exp(-b_0 t)}{b_0 (a_2 - b_0)} \right] \\
 \text{SIINFEKL}(t) &= a_1 \eta k_{21} v_0 \left[\frac{t - \tau}{a_1 b_0} + \frac{\exp(-a_1 (t - \tau)) - 1}{a_1^2 (b_0 - a_1)} - \frac{\exp(-b_0 (t - \tau)) - 1}{b_0^2 (b_0 - a_1)} \right] + a_2 \eta k_{22} v_0 \left[\frac{t - \tau}{a_2 b_0} + \frac{\exp(-a_2 (t - \tau)) - 1}{a_2^2 (b_0 - a_2)} - \frac{\exp(-b_0 (t - \tau)) - 1}{b_0^2 (b_0 - a_2)} \right]
 \end{aligned}
 \tag{2}$$

After inhibition of protein synthesis ($t \geq T_c$)

$$\begin{aligned}
 \text{DRiP}^*(t) &= \text{DRiP}(T_c) \exp(-\gamma a_1 (t - T_c)) \\
 \text{GFP}^*(t) &= \text{GFP}(T_c) \exp(-(\gamma a_2 + k_3)(t - T_c)) \\
 \text{XGFP}^*(t) &= \text{GFP}(T_c) \exp(-\gamma a_2 (t - T_c)) \\
 &\quad [1 - \exp(-k_3(t - T_c))] + \text{XGFP}(T_c) \exp(-\gamma a_2 (t - T_c)) \\
 \text{SIINFEKL}^*(t) &= \begin{cases} t \leq T_c + \tau & \text{SIINFEKL}(t) \\ t \geq T_c + \tau & \text{SIINFEKL}(T_c + \tau) + \eta \text{DRiP}(T_c) \\ [1 - \exp(-\gamma a_1 (t - T_c - \tau))] + \eta (\text{GFP}(T_c) + \text{XGFP}(T_c)) \\ [1 - \exp(-\gamma a_2 (t - T_c - \tau))] \end{cases}
 \end{aligned}
 \tag{3}$$

where γ = relative reduction of protein degradation rate after inhibition of protein synthesis. In (II) the notation $X(T_c)$ indicates the concentration of metabolite X at time $t = T_c$ as calculated according to the relations (I).

Alternative modeling of the delay phase between proteolytic generation and presentation of an antigenic peptide

To account for the remaining discrepancy between simulated and measured time courses of peptide presentation, the kinetic model was modified to take into account in a more realistic manner that the peptide after its proteolytic generation (by the proteasome or other protease) has to pass a number of consecutive processing steps before reaching the cell surface: protein $\rightarrow X_1 \rightarrow X_2 \rightarrow \dots \rightarrow X_n \rightarrow$ presented peptide.

Here X_1, X_2, \dots, X_n symbolize intermediate pools of peptides and peptide-MHC complexes along the pathway leading from the protease to the cell surface. The last equation in system (1) describing the formation of a surface-presented peptide was replaced by the following coupled system of equations:

$$\begin{aligned}
 \frac{d}{dt}[X_1] &= \eta a_1 \text{DRiP}(t) + \eta a_2 (\text{GFP}(t) + \text{XGFP}(t)) \\
 \frac{d}{dt}[X_2] &= k ([X_1] - [X_2]) \\
 &\vdots \\
 \frac{d}{dt}[X_n] &= k ([X_{n-1}] - [X_n]) \\
 \frac{d}{dt}[\text{SIINFEKL}] &= k [X_n]
 \end{aligned}
 \tag{4}$$

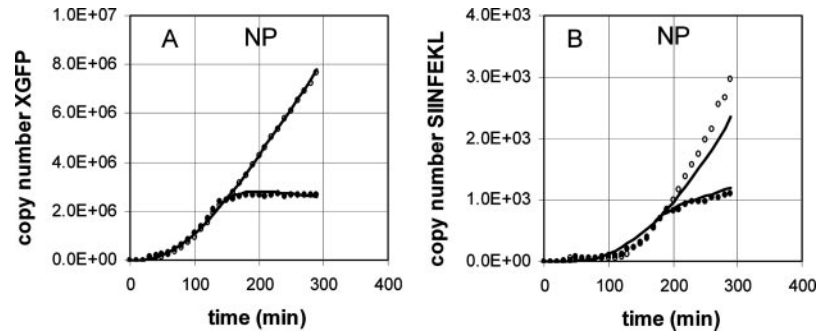
Here k is a universal rate constant representing the average flow of peptides through the endoplasmic and vesicular part of the presentation pathway.

Results

Numerical estimates of the model parameters were estimated by fitting time-dependent solutions (2) – (3) of equation system (1) to experimental progress curves. Data fitting was performed under Microsoft Excel using a nonlinear regression method (Solver 5.5 for Excel; Frontline Systems). To avoid over-fitting and to keep the number of freely adjustable parameters as small as possible, we took into account that owing to the similarity in length and sequence of the used protein constructs some of the model parameters should have very similar values in all experiments simulated. Accordingly some model parameters or combinations of them were forced to the same value for all experiments (indicated by only one value in the last column of Table II). The degradation rate of the DRiPs pool was set to $a_1 = 4.62 \times 10^{-2}$ min corresponding to a half-life of 15 min.

In a first series of calculations, we estimated numerical values of the model parameters by fitting the theoretical expressions to the measured time courses of cellular proteins and antigenic peptides. Based on the obtained best-fit parameter estimates, the majority of model curves were in good concordance with the measured time courses, but some curves showed larger deviations. For example, whereas the time course of the construct NP was well described by the model, the time course of the antigenic peptide derived from this construct in the absence of the protein synthesis inhibitor was systematically below the measured time course (cf, Fig. 2). Considering the simplicity of the kinetic model one should not be worried too much about this discrepancy. Our first idea was that the remaining discrepancies between theoretical and experimental time courses are due to an oversimplified description of the intermittent reaction steps taking place between excision of the antigenic peptide from the protein and its arrival on the cell surface. In fact, this part of the presentation pathway includes several successive reaction steps such as, for example, transport of the peptide into the ER, binding of the MHC class I complex in the ER and transport of the peptide-MHC complex along the vesicular pathway (17). Along this route several pools of intermediates in the ER and the Golgi system exist that are occupied by “just on their way” antigenic peptides. Filling of these pools in an early phase of the

FIGURE 2. Copy numbers of proteins and presented epitopes for the chimeric protein NP. The experimental data points were taken from Princiotta et al. (16). The solid curves represent best-fit solutions of the kinetic model without change of the degradation rates a_1 and a_2 within the time period after administration of the translation inhibitor cycloheximide.



transfection experiment could influence the delay kinetics observed for the presented epitope. We thus modified the kinetic model by replacing in the last equation in system (1) the term with the delayed time argument by a set of additional kinetic equations (see Equation 4) to describe in a more realistic manner the transition between protein degradation and formation of surface-presented antigenic peptides. However, this extension of the model did not resolve the systematic differences remaining in some cases between observed and simulated progress curves.

After a number of further unsuccessful attempts to improve the kinetic model, we noticed that a significantly better description of the data was obtained when we made the assumption that the rate of protein degradation is coupled with the rate of protein synthesis. Diminishing the value of the rate constants a_1 and a_2 for protein degradation by the factor $\gamma = 0.35$ within the time interval after inhibition of protein synthesis removed most of the discrepancies between theoretical and experimental progress curves and reduced the sum of deviation squares between experimental and theoretical curves by $\sim 50\%$ (see Fig. 2). As discussed in detail below, such an adjustment is in line with numerous reports in the literature (18–24), wherein the use of protein synthesis inhibitors has a direct effect on protein degradation. The best-fit parameter values obtained with this model variant are depicted in Table II (last column). From these parameter values the following conclusions can be drawn.

1) The estimated rate of protein synthesis amounts to $v_0 (k_{21} + k_{22})$ 472 copy numbers per minute. The length of the constructs is ~ 700 amino acid residues, corresponding to 2100 coding nucleotides of the mRNA. With an average transcription rate of 70 nucleotides per second (25) and an average translation rate of 7 peptide bonds per second about one protein copy would be synthesized by a single ribosome per minute. The estimated synthesis rate of 472 copy numbers per minute is more than two orders of magnitude higher. This points to a very efficient promoter used,

multiple translation of a single mRNA by polysomes, and possibly the existence of multiple genes.

2) The estimated degradation rate of the mRNA is $b_0 = 5 \cdot 10^{-3} \text{ min}^{-1}$ which is equivalent with a half-life of $\ln(2)/b_0 = 138 \text{ min}$. This indicates a high stability of the mRNA considering that the range of mRNA half-lives spans from some minutes to several hours (26).

3) The time delay between production of the antigenic peptide (or, more likely, production of an N-terminally extended precursor peptide (27)) and its appearance on the cell surface was estimated to $\tau = 40.5 \text{ min}$. This surprisingly long time delay must be due to the processing steps occurring in the ER and along the vesicular pathway as the life span of peptides in the cytosol was reported to lie in the range of seconds (28). If the above numerical value of the delay time for peptide traffic holds approximately true *in vivo*, we have to anticipate the earliest possible appearance of sizeable amounts of a virus-derived antigenic peptide about half an hour after onset of infection. Such a delay is in concordance with the observation that CD8⁺ T cells specific for nucleocapsid protein lysed cells that had been synthesizing nucleocapsid protein for $< 45 \text{ min}$ (29).

4) According to our computations the activation of GFP from the nonfluorescent to the fluorescent form proceeds with a half-life of $\ln(2)/k_3 = 12.2 \text{ min}$. This estimated value of the activation time is shorter than the value of 30 min given by Princiotta et al. (16), which was directly deduced from the time shift between the peaks of maximal protein production observed with radiolabeled and fluorescent protein. The apparent discrepancy between these numerical values is of methodological nature and demonstrates the advantage of a quantitative model. With the value of the parameter k_3 given in Table II, the time shift between the peaks of the simulated time courses of GFP and XGFP indeed amounts to 30 min, demonstrating that for kinetic reasons the time shift between these peaks is not identical with the half-life of fluorescence activation.

Table II. Parameters of the kinetic model used to simulate time courses of cellular protein levels and surface-presented antigenic peptides (16)

Parameter	Dimension	Meaning	Numerical Value		
			NP	KEKE	R-NP
b_0	min^{-1}	Degradation rate of mRNA		5.02×10^{-3}	
k_3	min^{-1}	GFP fluorescence activation rate		5.69×10^{-2}	
$v_0 (k_{21} + k_{22})$	min^{-1}	Rate of protein synthesis		4.72×10^2	
η		Presentation efficiency		1.08×10^{-3}	
a_1	min^{-1}	Degradation rate of DRiP		4.62×10^{-2}	
γ		Reduction factor for the rate constants k_{21} and k_{22} after inhibition of protein synthesis		3.50×10^{-1}	
τ	min	Delay time between generation of antigenic peptide and 1st appearance at cell surface		4.05×10^1	
a_2	min^{-1}	Degradation rate of native protein	2.78×10^{-3}	1.58×10^{-2}	5.72×10^{-2}
$v_0 k_{21}$	min^{-1}	Synthesis rate of DRiP	4.43×10^1	5.75×10^1	4.03×10^1
$v_0 k_{22}$	min^{-1}	Synthesis rate of native protein	4.28×10^2	4.15×10^2	4.32×10^2

5) The presentation efficiency was estimated to $\eta = 1.08 \cdot 10^{-3}$, i.e., $1/\eta = 930$ proteins have to be degraded to yield on the average a single presented Ag. This model-based value is close to the value of 994 degraded proteins per single antigenic peptide given by Princiotta et al. (16) and lies just between the reported minimal and maximal number of 100 and 10,000 proteins (30, 31) that have to be degraded for yielding on the average a single presented epitope.

6) As outlined above, the quality of the data fit significantly improved when we introduced a reducing factor γ with which the protein degradation rate constants a_1 and a_2 —independent from the specific protein considered (!)—are to be adjusted after administration of the protein synthesis inhibitor cycloheximide. The estimated value of $\gamma = 0.35$ means that the protein degrading capacity of the cell drops down to $\sim 35\%$ of its original value upon inhibition of protein synthesis.

7) Based on the estimated values of the degradation constant a_2 the half-lives ($= \ln(2)/a_2$) of the constructs NP, KEKE, and recombinant NP with Arg as N-terminal residue (R-NP) are 249, 44, and 12 min. These half-lives correlate well with the previously reported values given in Table I.

8) We have decomposed the calculated time courses of surface-presented antigenic peptides (SIINFEKL) (also shown in Fig. 3, B, D, and F) in Fig. 4 into the two contributions originating from the DRiP pool and the native protein. It is seen that the contribution of the DRiP-derived epitope prevails only for the stable construct NP and only within a short time interval between 50 and 100 min after start of transfection. Regarding the other two constructs, the fraction of antigenic peptides derived from the native protein clearly dominates over the whole time scale. Even for the stable construct NP the generation of antigenic peptides derived from DRiPs only marginally shortens the critical time span between onset of transfection and appearance of sizeable peptide amounts on the cell surface. This shows that the relative importance of DRiP-derived epitopes for the rapid recognition of infected cells depends strongly upon the life span of the native protein. Based on the numerical values given in Table II, we have simulated time courses of surface-presented epitopes at varying half-lives of the donating protein (see Fig. 5). For a very stable protein with a half-life of 10,000 min (≈ 7 days) during a time span of ~ 300 min after infection the surface pool of presented epitopes should almost exclusively originate from DRiPs provided that the parameters of the kinetic model reflect a typical *in vivo* situation.

9) According to the estimated values of the rate constants k_{21} and k_{22} for the synthesis of DRiPs and native protein the relative

DRiP rate, i.e., the share of DRiPs production in the total protein synthesis, amounts consistently to $\sim 10\%$ for the three constructs considered in our model simulations. This estimated DRiP rate is significantly lower than a rate of “upwards 35%” reported by Princiotta et al. (16) and other studies (32).

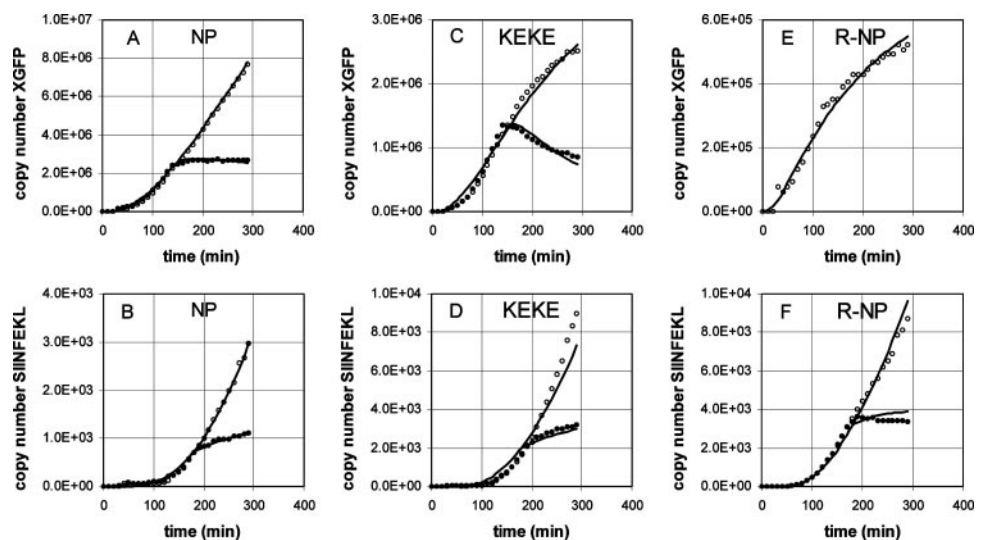
Discussion

The objective of this study was to perform an accurate quantification of the rates of the major processes involved in the cellular protein turnover and the production of Ags from endogenous proteins. Our main concern was to derive from existing data reliable quantitative figures that allow judging the production rate of so-called DRiPs and their effective contribution to the production of presented antigenic peptides. A quantification of the various kinetic processes underlying the cellular protein turnover and the MHC class I-mediated presentation of antigenic peptides is hardly possible without kinetic modeling. To this end, we have developed a mathematical model that despite its simplicity provides a very good description of the examined experiments.

One intriguing result of our computations is that the DRiP rate for the proteins tested in the transfection experiment is hardly larger than 10%. Nevertheless, as shown by our simulations, even a DRiP rate as low as 10% is sufficient to account for the observed kinetics of Ag presentation. A DRiP rate of $\sim 10\%$ is in clear contrast to a value of upwards of 35%, which has been estimated from the accumulation of radiolabeled proteins in the presence of proteasome inhibitors (15). This considerable discrepancy is possibly due to the fact that addition of the proteasome inhibitor disturbs abruptly the balance between protein synthesis and protein degradation. This leads to a sudden increase of the intracellular protein level exceeding the capacity of the folding machinery (33). Hence, a larger fraction of newly synthesized proteins fail to fold properly and contribute to the DRiP pool. In other words, it cannot be excluded that total and sudden inhibition of the cellular protein degradation provokes a higher fraction of DRiPs and thus leads to an overestimation of the DRiP rate present under normal physiological conditions.

In our opinion, a DRiP rate of $\sim 10\%$ instead of upwards of 35% seems to be feasible for several reasons. If DRiPs—as indicated by their naming—deviate in their amino acid sequence and conformation from those of native proteins, their production bears the risk of causing cell damage because a cell will hardly be able to cope with all possible abnormal variants of proteins and peptides. Moreover, the fraction of Ags presented on the cell surface under

FIGURE 3. Copy numbers of proteins and presented epitopes for the three chimeric protein constructs. The experimental data points were taken from Princiotta et al. (16). The solid curves represent best-fit solutions of the kinetic model if the protein degradation rate is reduced by the factor $\gamma = 0.35$ for the time period after administration of the translation inhibitor cycloheximide. The kinetic parameters used for the construction of these theoretical curves are depicted in Table II.



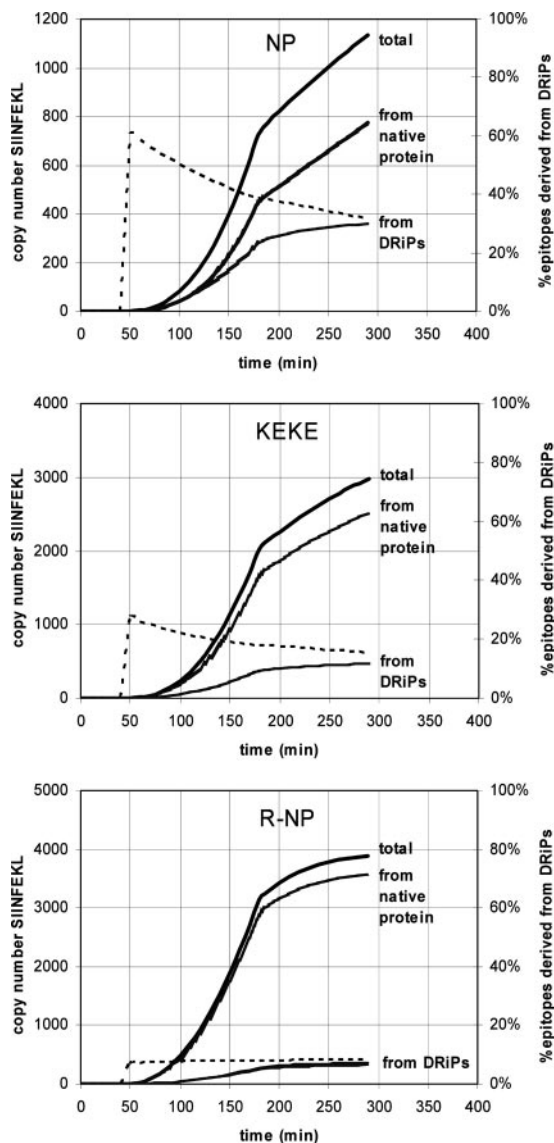


FIGURE 4. Contribution of DRiPs and native proteins to the pool of presented epitopes. The theoretical curves for the time-dependent formation of presented epitopes excised from DRiPs and the native protein are given by the two terms constituting the expressions (2) and (3) given in *Materials and Methods*. The dotted lines indicate the relative share of DRiP-derived epitopes.

stationary conditions, i.e., at balanced appearance and removal of MHC class I complexes, correlates with the DRiP rate. Hence, a DRiP rate of 35% and higher would imply the self-recognition by the T cells of the immune system to depend delicately on the safe generation of DRiPs. Is it really affordable to base 35% of correct self-recognition on a process that is regarded to be stochastic, i.e., to arise from imperfections of the cellular protein-synthesizing machinery?

According to our calculations and in accordance with the estimate given by Reits et al. (14), the presentation efficiency η of the epitope (SIINFEKL) is $\sim 10^{-3}$, i.e., on the average, 1000 proteins have to be degraded to yield a single presented SIINFEKL peptide. This value lies just between the upper value of 10^{-2} (30) and the lower value of 10^{-4} (31) reported for the presentation efficiency. Such low presentation efficiencies result to a certain extent from the inefficient production of antigenic peptides. Cascio et al. (34) have estimated that only 6–8% of the times that protein (= OVA)

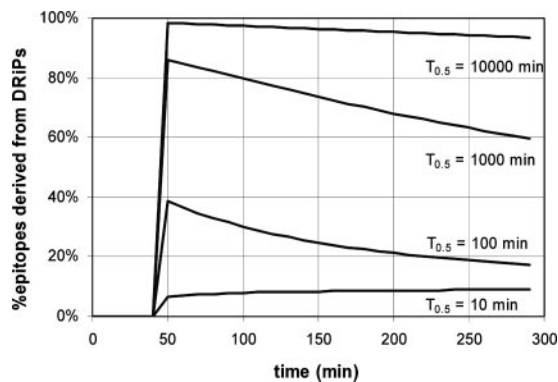


FIGURE 5. Contribution of DRiPs and native proteins to the pool of presented epitopes for different half-lives of the native protein. The theoretical curves were constructed with the parameter values given in Table II and at various half-lives of the native protein indicated.

molecules were digested was a SIINFEKL or an N-extended version produced. On top of that, there appears to be a substantial loss of potential epitopes and epitope precursors on their way from the cytosol to the cell surface. In living cells, cytosolic aminopeptidases remove one residue every 2–3 s (28). The cytosolic endopeptidase thimet oligopeptidase seems to have a particularly important role in destroying potential antigenic peptides that are generated by proteasomes (35). Therefore, most peptides generated by the proteasome get destroyed before reaching the ER (28). Moreover, aminopeptidases of the ER (36, 37) may also degrade epitopes before binding to the MHC complex. Considering the high risk for an epitope of being destroyed before reaching the cell surface it has been speculated that the proteasomal production of a larger variety of N-terminally extended epitope precursors is a means to protect the definitive epitope from the attack of aminopeptidases (27).

Our model-based simulations have clearly shown that the observed time courses with which the antigenic peptide (SIINFEKL) appeared on the cell surface required contributions from two protein pools—a pool of rapidly degraded proteins (in this work referred to as DRiPs although in the model just representing a fraction of proteins with a short half-life of ~ 15 min) and a pool of native proteins with significantly higher half-lives (NP and KEKE). A DRiP rate of $\sim 10\%$ was sufficient to account for the observed copy numbers of surface-presented epitopes. Based on the numerical values of the model parameters, one may interpolate that the contribution of DRiPs becomes indispensable for the rapid presentation of virus-derived antigenic peptides if the source proteins have half-lives of 15 h or higher (see Fig. 5). However, it has to be mentioned that the DRiP rate and the numerical values of the other parameters given in Table II were obtained under the premise that epitope generation proceeds with the same efficiency (η) from DRiPs and native proteins. This premise seems to be feasible because once unfolded by the 19S regulator and threaded into the interior of the proteasome the peptide chain should have lost its identity of stemming from a native or defective protein. However, it cannot be excluded that some differences in the efficiency of peptide generation remain because defective proteins may accumulate in special cellular compartments (e.g., PODs = oncogenic domains) where they are degraded by proteasomes (33). Peptides generated in such microcompartments may take different routes toward the cell surface than peptides generated in the cytosol and transported into the ER by TAP. To check the possible implications of differential presentation efficiencies, we have performed simulations where the ratio between the presentation efficiencies of

epitopes from DRiPs and native proteins was forced to either 0.1 or 10.0. In both cases, we were able to exactly reproduce the theoretical curves shown in Fig. 3, but the estimated synthesis rates of DRiPs changed inversely to the ratio of presentation efficiencies. At an assumed 10-fold higher presentation efficiency of DRiP-derived epitopes the synthesis rates of DRiPs from the constructs NP, KEKE, and R-NP dropped down to 1.2, 1.2, and 0.1%, respectively. Inversely, at an assumed 10-fold lower presentation efficiency of DRiP-derived epitopes, the synthesis rates of DRiPs from the constructs went up to 22, 35, and 47%. As expected, the available data does not allow discrimination between the two possible variants: 1) high presentation efficiency of DRiP-derived epitopes but very low DRiP rates around 1%; and 2) low presentation efficiency of DRiP-derived epitopes but high DRiP rates up to 50%.

The presence of cellular regulation mechanisms aiming at the homeostasis of the cellular protein pool may also account for our finding that inhibition of protein synthesis in HeLa cells by cycloheximide is very likely paralleled by a decline of the protein degradation rate. According to our calculations, the degradation rate of the protein constructs dropped to ~35% of the initial value immediately after inhibition of protein synthesis by cycloheximide. Obviously, the depletion of the cellular protein pool upon lowering or even completely blocking the rate of protein synthesis can be delayed by diminishing the rate of protein degradation. There is older literature (19, 38) indicating that rates of proteolysis decrease when protein synthesis is inhibited in bacteria and animal cells, especially in poor nutritional conditions. The first report on a dual inhibitory effect of cycloheximide appeared in 1969 (18). Succeeding studies pointed to an impact of cycloheximide on lysosomal protein degradation because the inhibitory effect on protein degradation correlated with the activity of some lysosomal cathepsins (20, 21). More recently, it was found that presence of cycloheximide led to the accumulation of polyubiquitinated murine μ chains in yeast *S. cerevisiae*. By contrast, degradation of carboxypeptidase Y was not impaired by cycloheximide, indicating that the drug effects a substrate-specific degradation step (22). The well-documented impact of cycloheximide on the protein-degrading capacity suggests the existence of a sensor, which enables the cell to monitor the rate of protein synthesis. It was hypothesized that this sensor consists of a protein that is permanently synthesized and in parallel degraded via the proteasome (24).

Taken together, there is a bulk of experimental evidence pointing to a coupling between the rates of protein translation and protein degradation, a fact that may have far reaching consequences for the interpretation of experiments where inhibitors of protein synthesis are applied to study interrelations between protein degradation and Ag production. For example, blocking of protein synthesis by cycloheximide resulted in a significant increase of the mobility of the TAP within a short time span of ~15 min (14). Based on the finding that the mobility of TAP increases when it is inactive and decreases when it translocates peptides, this increase in the mobility of TAP was accounted for by the disappearance of peptides generated from newly synthesized proteins. The conclusion was that freshly synthesized proteins are the major source for peptides transported by TAP. However, a general decline of the rate of protein degradation elicited by the complete blocking of protein synthesis would also imply a reduction of peptide generation and thus an increase in TAP mobility.

The main conclusions of this work are based on quantitative figures that have been obtained by application of a simple kinetic model. One might suspect that the simplicity and incompleteness of the used model restricts the credibility of our results. First, incomplete knowledge of the underlying molecular processes is al-

ways a problem in the interpretation of systemic data, regardless whether based on mathematical models or not. Second, simplicity of a model does not necessarily mean inadequacy (39). Lumping together individual reactions to a manageable number of overall reactions and describing their kinetics by mass action rate laws has often proved to provide a better quantitative description and understanding of the system's behavior than very detailed kinetic models that tend to fail if the kinetics of only one of the many included processes is not properly taken into account. Finally, the establishment of a more detailed kinetic model of the cellular protein turnover and of the Ag-presenting pathways is currently hampered by the insufficient kinetic characterization of the underlying processes.

Taken together, our computational analysis points to DRiP rates, which under conditions of a metabolic steady state are likely to be in the range of ~10%. The DRiP fraction of long-lived proteins with life spans of many hours is an indispensable source of epitopes during the early phase after onset of protein synthesis. It has been argued that errors in the synthesis of macromolecules are unavoidable thus accounting for the existence of DRiPs (32). However, by means of energy-dependent proofreading, cells are able to drop errors thresholds in the synthesis of nucleic acids to the order 10^{-9} and below, which is far below the level dictated by the laws of statistical physics. For example, DNA-based microbes have evolved a mechanism to yield a common spontaneous mutation rate of ~0.003 mutations per genome per replication (40). Therefore, it seems reasonable to speculate that the disadvantage of wasting at least 10% of the current protein production must be more than counterbalanced by the enormous advantage that results for the survival of higher organisms from an early detection of virus-infected or otherwise altered cells by the immune system.

Disclosures

The authors have no financial conflict of interest.

References

- Goldberg, A. L. 2003. Protein degradation and protection against misfolded or damaged proteins. *Nature* 426: 895–899.
- Ciechanover, A., and A. L. Schwartz. 2002. Ubiquitin-mediated degradation of cellular proteins in health and disease. *Hepatology* 35: 3–6.
- Nussbaum, A. K., T. P. Dick, W. Keilholz, M. Schirle, S. Stevanovic, K. Dietz, W. Heinemeyer, M. Groll, D. H. Wolf, R. Huber, et al. 1998. Cleavage motifs of the yeast 20S proteasome β subunits deduced from digests of enolase 1. *Proc. Natl. Acad. Sci. USA* 95: 12504–12509.
- Akopian, T. N., A. F. Kisselev, and A. L. Goldberg. 1997. Processive degradation of proteins and other catalytic properties of the proteasome from *Thermoplasma acidophilum*. *J. Biol. Chem.* 272: 1791–1798.
- Reits, E., J. Neijssen, C. Herberts, W. Benckhuijsen, L. Janssen, J. W. Drijfhout, and J. Neefjes. 2004. A major role for TPP1 in trimming proteasomal degradation products for MHC class I antigen presentation. *Immunity* 20: 495–506.
- Shastri, N., S. Schwab, and T. Serwold. 2002. Producing nature's gene-chips: the generation of peptides for display by MHC class I molecules. *Annu. Rev. Immunol.* 20: 463–493.
- Varshavsky, A., G. Turner, F. Du, and Y. Xie. 2000. Felix Hoppe-Seyler Lecture 2000: the ubiquitin system and the N-end rule pathway. *Biol. Chem.* 381: 779–789.
- Varshavsky, A. 1996. The N-end rule: functions, mysteries, uses. *Proc. Natl. Acad. Sci. USA* 93: 12142–12149.
- Grant, E. P., M. T. Michalek, A. L. Goldberg, and K. L. Rock. 1995. Rate of antigen degradation by the ubiquitin-proteasome pathway influences MHC class I presentation. *J. Immunol.* 155: 3750–3758.
- Khan, S., R. de Giuli, G. Schmidtke, M. Bruns, M. Buchmeier, M. van den Broek, and M. Groettrup. 2001. Cutting edge: neosynthesis is required for the presentation of a T cell epitope from a long-lived viral protein. *J. Immunol.* 167: 4801–4804.
- Yewdell, J. W., L. C. Anton, and J. R. Bennink. 1996. Defective ribosomal products (DRiPs): a major source of antigenic peptides for MHC class I molecules? *J. Immunol.* 157: 1823–1826.
- Turner, G. C., and A. Varshavsky. 2000. Detecting and measuring cotranslational protein degradation in vivo. *Science* 289: 2117–2120.
- Schild, H., and H. G. Rammensee. 2000. Perfect use of imperfection. *Nature* 404: 709–710.

14. Reits, E. A., J. C. Vos, M. Gromme, and J. Neeffjes. 2000. The major substrates for TAP in vivo are derived from newly synthesized proteins. *Nature* 404: 774–778.
15. Schubert, U., L. C. Anton, J. Gibbs, C. C. Norbury, J. W. Yewdell, and J. R. Bennink. 2000. Rapid degradation of a large fraction of newly synthesized proteins by proteasomes. *Nature* 404: 770–774.
16. Princiotta, M. F., D. Finzi, S. B. Qian, J. Gibbs, S. Schuchmann, F. Buttgerit, J. R. Bennink, and J. W. Yewdell. 2003. Quantitating protein synthesis, degradation, and endogenous antigen processing. *Immunity* 18: 343–354.
17. Kloetzel, P. M. 2004. The proteasome and MHC class I antigen processing. *Biochim. Biophys. Acta* 1695: 225–233.
18. Feldman, M., and G. Yagil. 1969. Does cycloheximide interfere with protein degradation? *Biochem. Biophys. Res. Commun.* 37: 198–203.
19. Goldberg, A. L., and A. C. St John. 1976. Intracellular protein degradation in mammalian and bacterial cells: part 2. *Annu. Rev. Biochem.* 45: 747–803.
20. Amenta, J. S., M. J. Sargus, and F. M. Baccino. 1978. Inhibition of basal protein degradation in rat embryo fibroblasts by cycloheximide: correlation with activities of lysosomal proteases. *J. Cell. Physiol.* 97: 267–283.
21. Wildenthal, K., and E. E. Griffin. 1976. Reduction by cycloheximide of lysosomal proteolytic enzyme activity and rate of protein degradation in organ-cultured hearts. *Biochim. Biophys. Acta* 444: 519–524.
22. Amshoff, C., H. M. Jack, and I. G. Haas. 1999. Cycloheximide, a new tool to dissect specific steps in ER-associated degradation of different substrates. *Biol. Chem.* 380: 669–677.
23. Lee, H. K., and L. Marzella. 1994. Regulation of intracellular protein degradation with special reference to lysosomes: role in cell physiology and pathology. *Int. Rev. Exp. Pathol.* 35: 39–147.
24. Gerlinger, U. M., R. Guckel, M. Hoffmann, D. H. Wolf, and W. Hilt. 1997. Yeast cycloheximide-resistant crl mutants are proteasome mutants defective in protein degradation. *Mol. Biol. Cell* 8: 2487–2499.
25. Lyakhov, D. L., B. He, X. Zhang, F. W. Studier, J. J. Dunn, and W. T. McAllister. 1998. Pausing and termination by bacteriophage T7 RNA polymerase. *J. Mol. Biol.* 280: 201–213.
26. Czaplinski, K., M. J. Ruiz-Echevarria, C. I. Gonzalez, and S. W. Peltz. 1999. Should we kill the messenger? The role of the surveillance complex in translation termination and mRNA turnover. *BioEssays* 21: 685–696.
27. Peters, B., S. Bulik, R. Tampe, P. M. Van Endert, and H. G. Holzhtuter. 2003. Identifying MHC class I epitopes by predicting the TAP transport efficiency of epitope precursors. *J. Immunol.* 171: 1741–1749.
28. Reits, E., A. Griekspoor, J. Neijssen, T. Groothuis, K. Jalink, P. van Veelen, H. Janssen, J. Calafat, J. W. Drijfhout, and J. Neeffjes. 2003. Peptide diffusion, protection, and degradation in nuclear and cytoplasmic compartments before antigen presentation by MHC class I. *Immunity* 18: 97–108.
29. Esquivel, F., J. Yewdell, and J. Bennink. 1992. RMA/S cells present endogenously synthesized cytosolic proteins to class I-restricted cytotoxic T lymphocytes. *J. Exp. Med.* 175: 163–168.
30. Villanueva, M. S., P. Fischer, K. Feen, and E. G. Pamer. 1994. Efficiency of MHC class I antigen processing: a quantitative analysis. *Immunity* 1: 479–489.
31. Montoya, M., and M. Del Val. 1999. Intracellular rate-limiting steps in MHC class I antigen processing. *J. Immunol.* 163: 1914–1922.
32. Yewdell, J. W., E. Reits, and J. Neeffjes. 2003. Making sense of mass destruction: quantitating MHC class I antigen presentation. *Nat. Rev. Immunol.* 3: 952–961.
33. Anton, L. C., U. Schubert, I. Bacik, M. F. Princiotta, P. A. Wearsch, J. Gibbs, P. M. Day, C. Realini, M. C. Rechsteiner, J. R. Bennink, and J. W. Yewdell. 1999. Intracellular localization of proteasomal degradation of a viral antigen. *J. Cell Biol.* 146: 113–124.
34. Cascio, P., C. Hilton, A. F. Kisselev, K. L. Rock, and A. L. Goldberg. 2001. 26S proteasomes and immunoproteasomes produce mainly N-extended versions of an antigenic peptide. *EMBO J.* 20: 2357–2366.
35. York, I. A., A. X. Mo, K. Lemerise, W. Zeng, Y. Shen, C. R. Abraham, T. Saric, A. L. Goldberg, and K. L. Rock. 2003. The cytosolic endopeptidase, thimet oligopeptidase, destroys antigenic peptides and limits the extent of MHC class I antigen presentation. *Immunity* 18: 429–440.
36. Serwold, T., F. Gonzalez, J. Kim, R. Jacob, and N. Shastri. 2002. ERAAP customizes peptides for MHC class I molecules in the endoplasmic reticulum. *Nature* 419: 480–483.
37. York, I. A., S. C. Chang, T. Saric, J. A. Keys, J. M. Favreau, A. L. Goldberg, and K. L. Rock. 2002. The ER aminopeptidase ERAAP1 enhances or limits antigen presentation by trimming epitopes to 8–9 residues. *Nat. Immunol.* 3: 1177–1184.
38. Poole, B., and M. Wibo. 1973. Protein degradation in cultured cells: the effect of fresh medium, fluoride, and iodoacetate on the digestion of cellular protein of rat fibroblasts. *J. Biol. Chem.* 248: 6221–6226.
39. May, R. M. 2004. Uses and abuses of mathematics in biology. *Science* 303: 790–793.
40. Drake, J. W. 1991. A constant rate of spontaneous mutation in DNA-based microbes. *Proc. Natl. Acad. Sci. USA* 88: 7160–7164.